Nanofibrous Adhesion: The Twin of Gecko Adhesion

Guangming Gong,[†] Chen Zhou,[†] Juntao Wu,[*,†] Xu Jin,[†,§] and Lei Jiang[‡,†]

[†]Key Laboratory of Bio-Inspired Smart Interfacial Science, Technology of Ministry of Education, School of Chemistry and Environment, Beihang University, Beijing 100191, P.R. China, [§]Research Institute of Petroleum Exploration & Development, China National Petroleum Corporation, Beijing 100191, P.R. China, and [‡]Beijing National Laboratory for Molecular Sciences, Institute of Chemistry, Chinese Academy of Sciences, Beijing 100191, P.R. China

ABSTRACT Inspired by dusty spider dragline silk, we studied the adhesive interaction between artificial nanofibers and their aerosol surroundings. The nanofibers are found to be able to actively capture particulate matters from the environment, exactly as the spider dragline silk does. Examinations prove that such nanofibrous adhesion is insensitive to the chemical nature of the fibers and the physical states of the particulate matter and depends only on the fiber diameters. Such facts indicate that nanofibrous adhesion is a case of dry adhesion, mainly governed by van der Waals force, sharing the same mechanism to gecko adhesion. Nanofibrous adhesion is of great importance and has promising potential. For instance, in this work, nanofibers are fabricated into a thin and translucent filter, which has a filtration performance, as high as 95%, that easily outperformed ordinary ones. We believe that this adhesive property of nanofibers will open up broader applications in both scientific and industrial fields.

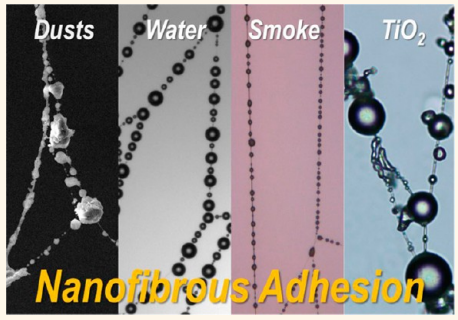

KEYWORDS: adhesion · polymeric nanofibers · fine particulate matters · dry adhesion

Nanofibers have gained intensive attention in the past decades. Compared with conventional fibers, nanofibers have a unique advantage due to their dramatically reduced diameters, which give them extremely large aspect ratio and higher orientation on molecular levels.[1,2] These priorities make nanofibers super-candidates to be studied and applied in advanced composites, tissue engineering, sensors, modern pharmacology, advanced electronics, *etc.*[3−10] On the other hand, the stickiness of nanofibers is an important and interesting aspect.[11−15] Inspired by biofibrous systems,[13−15] the adhesion between fibers and substrates are extensively studied. For instance, the ability of the gecko to climb swiftly on the vertical smooth surfaces originates from the micro hierarchy of its toes, as shown in Figure 1A−E. When walking, the integrated van der Waals force generated between the setae tip and the flat surface are mighty enough to sustain a gecko's body weight.[16,17] This tip-to-substrate dry adhesion is considered to be the legacy of nature's revolutionary nanotechnology, which has inspired human beings to develop marvelous inventions.[18−20]

However, the tip-to-substrate adhesion is not sufficient to illustrate the full picture of the adhesion of nanofibers. Actually, Mother Nature's legacy not only makes the nanofibers' tip adhesive, but the whole length as well. One vivid case is dusty spider silk. If exposed to air for long enough, the entire spider web could be dusty, both the viscoelastic viscid silk[21−23] and the backbone of the draglines, as shown in Figure 1G. Specifically, the dragline silk, which is famous for mechanical performance instead of viscosity, is also found to be dusty. Close observations (Figure 1H) of a dusty dragline reveal that numerous tiny dust particles can attach firmly on its surface, suggesting that thin spider silk can be sticky to tiny particles even without the help of the glycoprotein glue droplets.[23] Interestingly, such harvesting ability has also been unintentionally reported on "non-sticky" artificial nanofibers.[24,25] We speculate that there should be some hidden and universal reason determining this fiber-to-particles adhesion on different types of nanofibers, even while there has been no explicit statement on the mechanism of such adhesive behaviors. In this work, we would like to further investigate the deeper merit of these phenomena and reveal their secrets.

* Address correspondence to wjt@buaa.edu.cn.

Received for review November 5, 2014 and accepted January 20, 2015.

Published online January 20, 2015
10.1021/nn5063112

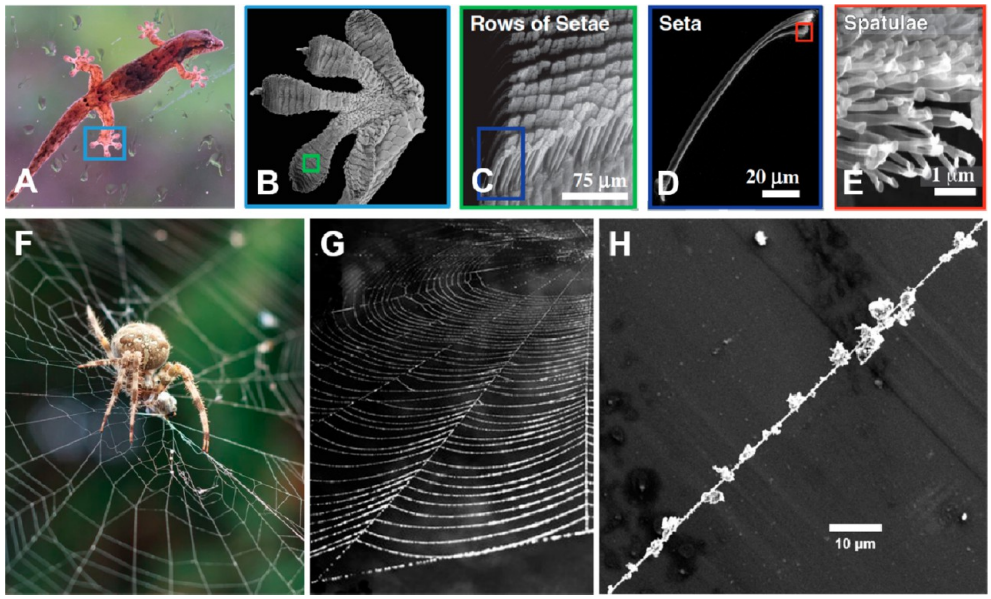

Figure 1. Gecko adhesion *vs* the nanofibrous adhesion discovered on spider dragline silk. (A–E) Characterizations of a gecko's toes, revealing its secret of climbing on vertical smooth glass. (C–E) are reproduced with permission from ref 16. Copyright 2000. Nature Publishing Group. (F) A digital picture of a spider fixing its web. Photo courtesy of ©Igor Klajo. (G) If exposed to air for long enough, the entire spider web will become dusty, including not only the viscid silk but also the draglines. Photo courtesy of ©Stephanie Rousseau. (H) A strand of unfresh spider dragline silk observed under SEM, displaying numerous tiny dust particles adhering on the string.

RESULTS AND DISCUSSION

To mimic the adhesion of the spider dragline silk, artificial polymeric nanofibers with the same diameter scale were produced *via*, electrospinning. The as-prepared neat electrospun polyimide (PI) nanofibers were placed into the same atmosphere where the spider fibers were collected to investigate the artificial nanofibers' adhering ability. After the fibers were placed into the open air, the surficial morphologies of natural spider silks and artificial nanofibers were characterized. The nanofibers behaved exactly as the spider webs did (shown in Figure 2). Because the surface of the PI nanofibers was dry and smooth, some certain force should be responsible for securing the air-borne tiny particulate matter when air flowed around the freshly obtained nanofibers. This force accounted for the essence of such adhesive behavior. On the basis of our observation, such nanofiber-to-particle adhesion took place quite effectively, especially in heavy polluted air conditions. Because the $PM_{2.5}$ concentration 300 $\mu g/m^3$ is considered as the indicator of "serious pollution" in air quality index (AQI) reports, so we tested the PI nanofibers' adhesion state to air-borne fine particles on a heavy smog day (AQI: 381 $\mu g/m^3$). It took the nanofibers less than 5 min to harvest $PM_{2.5}$ particles to saturation. However, as a comparison, although treated in the same condition and with same amount of time, there were barely any tiny particles attached to the thick fiber, as Figure 2F presents. It indicated that such adhesive efficiency was dependent on the fiber diameter. As a result, the adhesion between particulate matter and the nanofibers was in turn termed 'nanofibrous adhesion'. However, the mechanism of nanofibrous adhesion needs further explanation.

In the following steps, several different aerosol atmospheres were built for the polyimide nanofibers to conduct their nanofibrous adhesion so that the influence of the chemical composition and physical state of the particles on the adhesive mechanism could be studied. The particulate environment included fog (ultrafine water droplets), cigarette smoke and an aerosol of TiO_2. The fog condensed onto the strings to form a beautiful pearl-necklace-like configuration. The cigar smoke, majorly containing gas-state coal-tar, assembled into similar shapes as well. The TiO_2 aerosol formed from liquid $TiCl_4$ also assembled into beaded string structures. The results are shown in Figure 3A–D, proving that polyimide nanofibers were able to secure more tiny particulate substances than merely air-borne dust, as demonstrated in Figure 3A. In addition, given that the air-borne dust was a mixture of multiple types of particulate matters, the chemical composition and physical states of the surrounding aerosol had no major impact on the effectiveness of nanofibrous adhesion.

Other types of polymeric nanofibers with different chemical compositions were examined in the same atmospheres, including materials with low surface free energies, *e.g.*, polyvinylidene fluoride (PVDF) and polystyrene (PS), and high surface free energies, *e.g.*, polyurethane (PU), poly(vinyl alcohol) (PVA), and poly(ethylene oxide) (PEO). It turned out that the nanofibrous adhesion would eventually occur, despite the

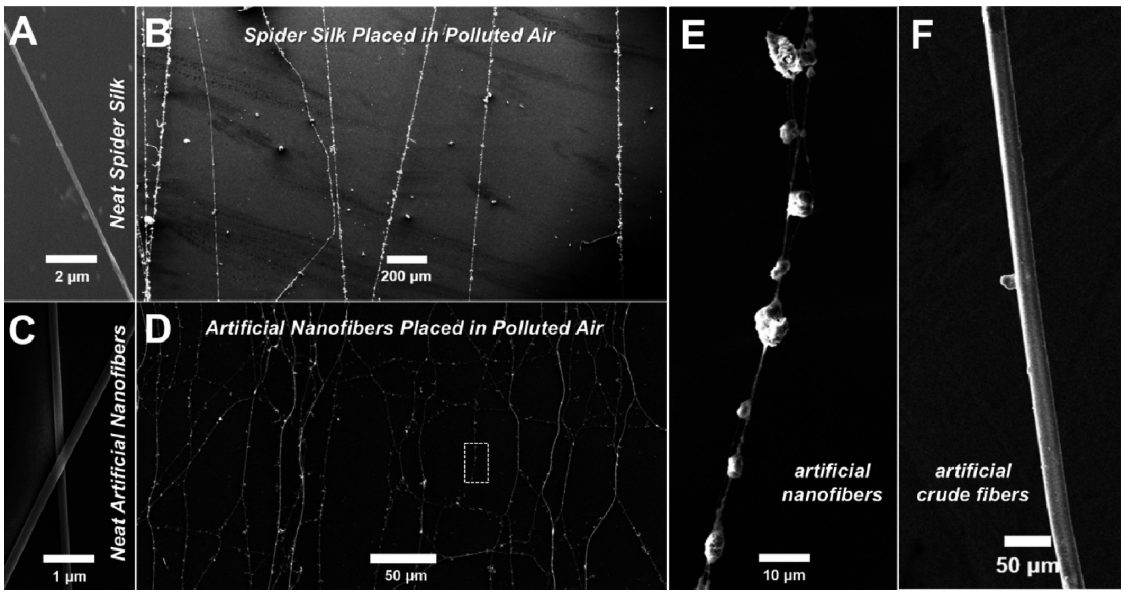

Figure 2. Using electrospun polyimide nanofibers to mimic the adhesion behaviors of the spider silk. (A) Characterization of the freshly obtained spider dragline silk; (B) characterization of the spider dragline silks placed in open air. Plenty of dust particles were adhering on the bionanofibers. (C) Characterization of neat polyimide nanofibers; (D) characterization of electrospun polyimide fibers after being placed in open air. Each thin thread captured a full string of airborne fine particulate matters. (E) Specified study of a single artificial nanofiber adhering multiple dust particles. Specified characterization of single spider fiber can be referred to Figure 1H. (F) As a comparison, a thick crude PI fiber with a diameter of 28 μm was also tested to investigate its adhesion to air-borne dust particles. Although the exposure time to air was equal to that of the nanofibers, there were barely any particles attached on it.

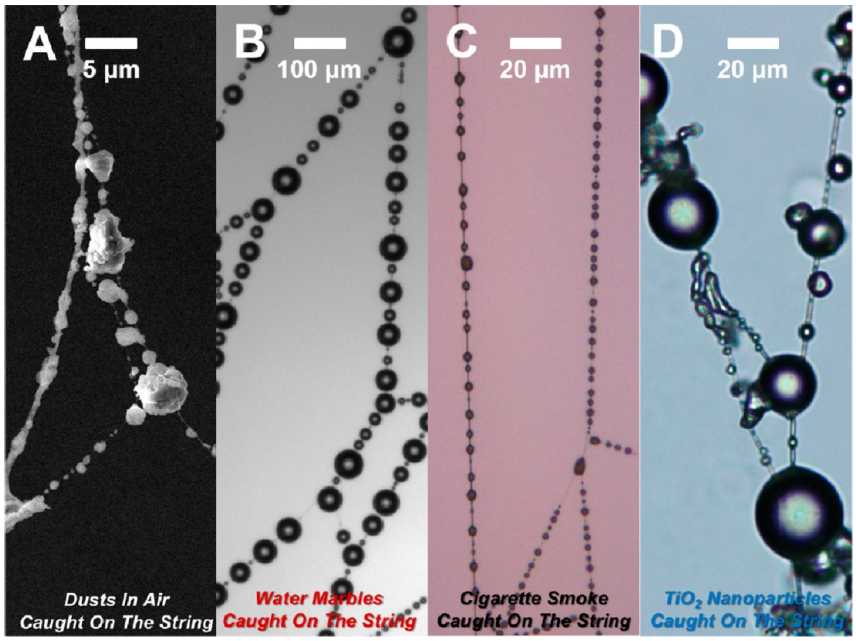

Figure 3. Particulate substances caught on the polyimide nanofibers from different atmospheres. (A) SEM characterization of dust particles caught on the nanostrings from the polluted air in Beijing; (B) water marbles caught on nanofibers from water steam; (C) cigarette smoke condensed on the nanofibers; (D) TiO_2 particles assembled on the nanostrings.

distinctive chemical natures of the nanofibers. Additionally, the polymeric nanofibers' adhesion to different types of particles with distinctive physical states or chemical compositions was also tested. The adhesions were recorded and categorized in Supporting Information Figure S1. Notably, inorganic carbon nanotubes[24] were also reported to be able to secure aerosol TiO_2 into shapes as Figure 3D demonstrated. Such facts strongly indicate that the nanofibrous adhesion is universal and not strongly affected by the surficial chemical composition of the nanofibers.

Although the nanofibrous adhesion was universal, the adhesion efficiencies varied across nanofibers with different diameters (also seen in the comparison

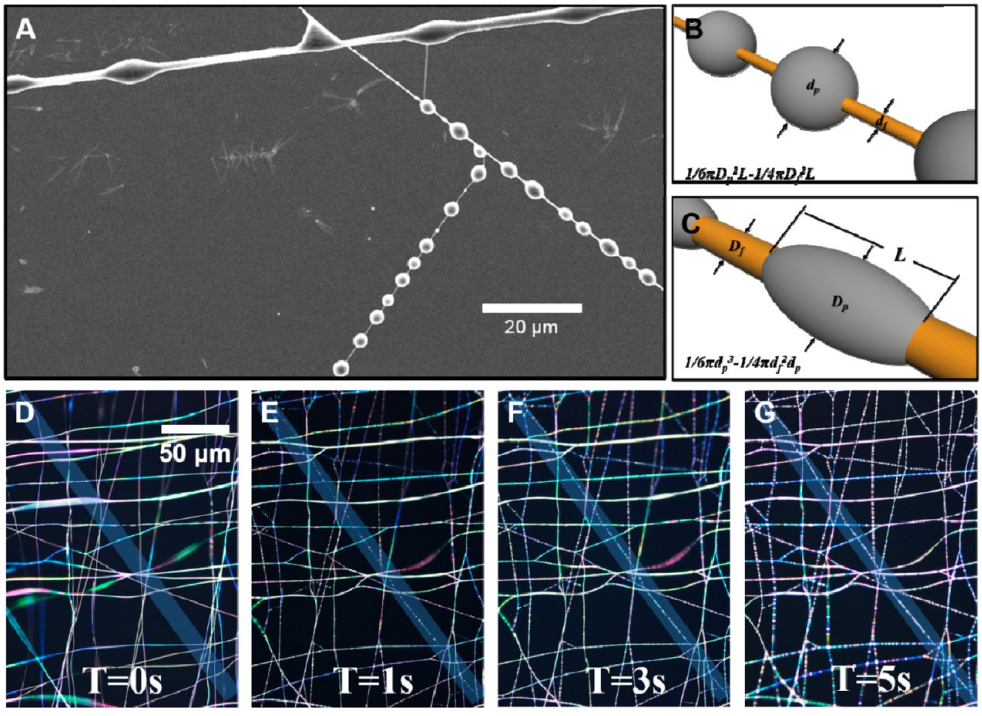

Figure 4. Adhering ability variations caused by the fiber diameters. (A) SEM characterization of three nanostrings with different diameters and cigar smoke catching efficiency. (B and C) Computational graphics simulating the adhesion states on thin and thick fibers, respectively. (D−G) The smoke-catching process directly observed under an optical microscope. The *in situ* observation indicated that the deposition rate of the smoke was faster on the thinner fiber than that on the thicker fiber. And the smoke deposition process was considerably fast.

between Figure 1, panels E and F). The diameters' influence on the nanofibrous adhesion was investigated. We utilized the instability[26] of electrospinning to obtain thick and thin nanofibers of the same type and studied their adhesive properties simultaneously. Figure 4A is a snapshot of three polyimide nanostrings of different diameters. We recorded their efficiency in catching cigarette smoke. The efficiency of the smoke-catching was defined as 1) the volume ratio of the smoke droplets to the part of the fiber on which the smoke was deposited and 2) the distances between every pair of droplets. According to Figure 4A, the droplets on the thinner fibers tended to form more spherical structures than those on the thicker fibers. Figure 4B,C shows schematic illustrations of such a difference. The volume-to-fiber ratio of each case was calculated (see calculation in Supporting Information, Figure S2). According to calculation, thinner fibers were able to hold more smoke per unit volume than thicker fibers. In addition, the distances between each two adjacent droplets on thinner fiber were far smaller than on the thick fibers. It demonstrated that thin fibers possessed far more active sites than the thick fibers did. As a result, the thinner fibers were more efficient than the thicker fibers in adhering the smoke droplets. Furthermore, the fiber diameters also affected the deposition rate. By applying smoke to the nanofibrous mesh directly under an optical microscope, the adhering situations were recorded and are illustrated in Figure 4D−G. The smoke revealed an originally "invisible" ultrathin string due to the droplets caught on it (highlighted in the blue area), while other discernible fibers exhibited no or little changes. This means that the deposition rate on the thinner fibers was faster than on the thicker fibers.

Thus, far, we have been describing a nanofiber-to-particle adhesion behavior. Such adhesion is not strongly affected by the chemical composition or physical state of the fibers or aerosols, but they are dependent on the size of fiber diameter. These facts imply that the driving force of this adhesion majorly relies on the van der Waals forces. To further support this conclusion, we attempted to directly measure the adhesive force generated at the surface of nanofibers using a dynamic contact angle test system. The mechanism of the test is elaborated in Supporting Information, Figure S3. The detected adhesion between multiple types of thin fibers at the nano contact scale was in the range of approximately a few micro Newtons, as shown in Supporting Information Figure S4. This result is consistent with the previous works which had demonstrated that van der Waals force dominated in nanocontact situations.[16,17,11] As a result, the mechanism of such nanofibrous adhesion is actually in accordance with gecko adhesion, only the former behaves in a particle-to-fiber way and the latter in a tip-to-substrate way. This newly discovered behavior expands the

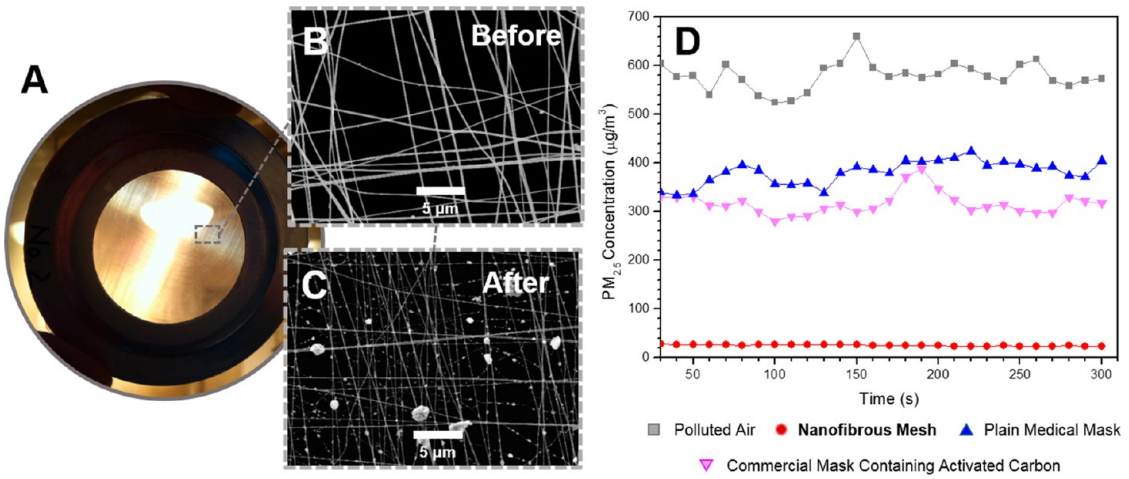

Figure 5. Prototype of the nanofibrous mesh for mitigating the $PM_{2.5}$ pollutant and the characterization of its effects. (A) Translucent orthogonal nanofibrous mesh collected on a metal loop; (B) SEM characterization of the mesh before filtration; (C) characterization of the mesh after filtration, presenting complex substances adhering on the fibers; (D) $PM_{2.5}$ concentrations of air treated by different filters, monitored by an aerosol monitor. The $PM_{2.5}$ mitigating effect of the nanofibrous mesh was exceptionally greater than that of the ordinary medical mask and the commercial anti-$PM_{2.5}$ masks containing activated carbons. Such effect was prominent, given that the nanomesh was far thinner than the masks.

knowledge of the dry adhesiveness of nanofibers and starts to reveal a more comprehensive understanding of the legacy of nature's revolutionary nanotechnology.

Such nanofibrous adhesive technology is expected to have meaningful and practical use. For instance, it can be used as an effective tool to harvest water from fog; there has been a report on using nanofibers as a precursor to collect water.[25] Additionally, nanofibrous adhesion can be developed to realize naked-eye-operation by visualizing ultrathin fibers as ref 24 suggested. Furthermore, as suggested by our observations in Figure 4, nanofibers also may be used in a next-generation cigarette filter to minimize the harm of tobacco to smokers. While the most intriguing and urgent field that nanofibrous adhesion can perform seems to be in the prevention of local air pollution in China. Accordingly, nanofibers can be utilized as novel and more effective filters to capture airborne pollutants and lower the concentration of the $PM_{2.5}$. In turn, one prototype of nanofibrous mesh was created in our laboratory, shown in Figure 5A. The translucent mesh was used as a filter to reduce the $PM_{2.5}$ concentration of the heavily polluted air; the starting $PM_{2.5}$ concentration exceeded 600 $\mu g/m^3$. The filtered air was examined by an aerosol monitor (see details in Methods). As a comparison, the filter efficiency of plain medical masks and commercial masks containing activated carbons were also detected. The results were plotted against time-lapse into Figure 5D after the concentration of $PM_{2.5}$ was steady. The results proved that the nanomesh's $PM_{2.5}$ mitigating effect outperformed the other two conventional types of masks. It was able to lower the $PM_{2.5}$ concentration to less than 25 $\mu g/m^3$ with a filtration efficiency greater than 95%. Given that the nanomesh was thin and transparent, the filtration performance of the nanomesh was worthy of higher expectations. The higher performance of the nanofibers came from the additional adhesive effect of the nanofibers. SEM characterizations before and after the filtration test are illustrated in Figure 5B,C. Although the pores of the mesh were larger than the particles' sizes, from Figure 5C, the nanostrings of the mesh could adhere the tiny particles, preventing them from penetrating through the pores. Additionally, by taking advantages of modern advanced polymers, such nanofilters are able to be applied beyond just ordinary cases. Taking polyimide nanofibers as an example, due to their high T_g, polyimide nanofibers could endure heat as high as 300 °C,[27,28] opening a door for them to be utilized as efficient thermally durable filters.

CONCLUSIONS

Inspired from dusty spider dragline silk, the interactions between tiny particles and nanofibers at the nano contact scale is studied and termed as the nanofibrous adhesion. Experiments prove that nanofibrous adhesion is not sensitive to the chemical composition of substances but only to the size of the nanofibers. The efficiency and sensitivity of nanofibrous adhesion are greatly affected by their diameters. On the basis of previous studies and combined with our own observations, we conclude that nanofibrous adhesion is majorly driven by the van der Waals force, similar to gecko adhesion. The study of nanofibrous adhesion completes the understanding and utilization of sticky properties of nanofibers. At the current state, an ultrathin lab-made model nanofilter exhibits a great filtration efficiency as high as 95%, presenting

the advantages of nanofibrous adhesion. Such nanofibrous adhesion endows a prominent future for the further development of nanofibers in both the scientific and industrial worlds.

METHODS

Sample Preparations. Polyimide (PI) was synthesized *via* a traditional two-step method. 4,4′-Oxidianiline (ODA) and pyromellitic dianhydride (PMDA) with equal amount of substance were condensationally polymerized in *N*,*N*-dimethylformamide (DMF) to form the precursor, polyamic acid (PAA/DMF). PAA/DMF (8 wt %) was electrospun at high voltage (Spellman Co. SL50P60) into nanofibers and collected on a U-shape metal frame. Then, the PAA nanofibers were thermally imidized to afford PI nanofibers. Other polymeric nanofibers were electrospun directly from their corresponding solutions. In electrospinning processes, polymer solutions were added in plastic syringes with a metal nozzle connected on its tip. High voltages were applied on the nozzle to generate nanofibers. The nanofibers were collected on the U-shape metal frames by swiping the frames swiftly across the spinning jet. Due to characters of different types of polymer solutions, certain parameters of electrospinning, *e.g.*, voltages, feeding rate, concentrations and viscosities of the solutions, were adjusted accordingly, in order to maintain the diameters of all the nanofibers into similar ranges. Then, the nanofibers were sealed and prepared for following procedures. Spider silks were obtained in the campus woods of Beihang University.

Capturing of the Particulare Matters. (1) Capture of air-borne $PM_{2.5}$: neat nanofibers were placed in the open air when hazes ($PM_{2.5}$ concentration exceeds 300 $\mu g/m^3$) took place. The exposure time was calculated to study how long would the nanofibrous adhesion take. (2) Capture of water: nanofibers were placed on a contact angle detector (Dataphysics, OCA20, Germany). Water steam was generated by a commercial steamer and the stream of humid was allowed to flow around the nanofibers. Water marbles caught on the strings were pictured by the detector's accompanying CCD. (3) Capture of cigarette smoke: the smoke of a cigar was allowed to flow through the nanofibers, similar to what was introduced in (2). (4) Capture of the TiO_2: a few drops of $TiCl_4$ (Sigma Aldridge) were added into a large beaker's bottom. Then, the beaker was canopied over the nanofibers. $TiCl_4$ would form TiO_2 nanoparticles when it contacts humid air, resulting in a fog of TiO_2 aerosol. The deposition process was similar to what was discussed in (1).

Characterizations. An FEI Quanta 200F scanning electronic microscopy was used to analyze the morphology of each sample. The observation of the spider silk used the low vacuum mode. Also, the samples' morphologies were studied by an optical microscope (Olympus, BX51, Japan). The *in situ* detection of the nanofibers catching cigarette smoke was also conducted on the optical microscope. A Dust Trak aerosol monitor (Model 8530, TSI, Inc.) was used to detect the concentrations of $PM_{2.5}$ in the air quality tests. Filters were covering the inlet of the machine and the filtered air was tested. Sampling frequency was 0.1 Hz.

Conflict of Interest: The authors declare no competing financial interest.

Supporting Information Available: (1) Multiple particulate matters captured by different types of polymeric fibers, (2) calculations of nanofibrous adhesion efficiency. This material is available free of charge *via* the Internet at http://pubs.acs.org.

Acknowledgment. The work is financially supported by the National Natural Science Foundation of China (No.51373007, 51003004), the Beijing Natural Science Foundation (No.2142019), the National Basic Research Program of China (No.2010CB934700, 2012CB933200), the Fundamental Research Funds for the Central Universities, and the SRF for ROCS, SEM.

REFERENCES AND NOTES

1. Silva, G. A.; Czeisler, C.; Niece, K. L.; Beniash, E.; Harrington, D. A.; Kessler, J. A.; Stupp, S. I. Selective Differentiation of Neural Progenitor Cells by High-Epitope Density Nanofibers. *Science* **2004**, *303*, 1352–1355.
2. Kakade, M. V.; Givens, S.; Gardner, K.; Lee, K. H.; Bruce Chase, D.; Rabolt, J. F. Electric Field Induced Orientation of Polymer Chains in Macroscopically Aligned Electrospun Polymer Nanofibers. *J. Am. Chem. Soc.* **2007**, *129*, 2777–2782.
3. Huang, Z. M.; Zhang, Y. Z.; Kotaki, M.; Ramakrishna, S. A Review on Polymer Nanofibers by Electrospinning and Their Applications in Nanocomposites. *Compos. Sci. Technol.* **2003**, *63*, 2223–2253.
4. Huang, J.; Virji, S.; Weiller, B. H.; Kaner, R. B. Polyaniline Nanofibers: Facile Synthesis and Chemical Sensors. *J. Am. Chem. Soc.* **2003**, *125*, 314–315.
5. Guo, X.; Ying, Y.; Tong, L. Photonic Nanowires: From Subwavelength Waveguides to Optical Sensors. *Acc. Chem. Res.* **2014**, *47*, 656–666.
6. Salgado, A. J.; Coutinho, O. P.; Reis, R. L. Bone Tissue Engineering: State of the Art and Future Trends. *Macromol. Biosci.* **2004**, *4*, 743–765.
7. Wang, X.; Drew, C.; Lee, S. Y.; Senecal, K. J.; Kumal, J.; Samuelson, L. A. Electrospun Nanofibrous Membranes for Highly Sensitive Optical Sensors. *Nano Lett.* **2002**, *2*, 1273–1275.
8. Long, Y. Z.; Yu, M.; Sun, B.; Gu, C. Z.; Fan, Z. Recent Advances in Large-scale Assembly of Semiconducting Inorganic Nanowires and Nanofibers for Electronics, Sensors and Photovoltaics. *Chem. Soc. Rev.* **2012**, *41*, 4560–4580.
9. Sill, T. J.; von Recum, H. A. Electrospinning: Applications in Drug Delivery and Tissue Engineering. *Biomaterials* **2008**, *29*, 1989–2006.
10. Ramakrishna, S.; Fujihara, K.; Teo, W. E.; Lim, T. C.; Ma, Z. *An Introduction to Electrospinning and Nanofibers*; World Scientific: Singapore, 2005.
11. Shi, Q.; Wan, K. T.; Wong, S. C.; Chen, P.; Blackledge, T. A. Do Electrospun Polymer Fibers Stick? *Langmuir* **2010**, *26*, 14188–14193.
12. Shi, Q.; Wong, S. C.; Ye, W.; Hou, J.; Zhao, J.; Yin, J. Mechanism of Adhesion Between Polymer Fibers at Nanoscale Contacts. *Langmuir* **2012**, *28*, 4663–4671.
13. Autumn, K.; Peattie, A. M. Mechanisms of Adhesion in Geckos. *Integ. Comp. Biol.* **2002**, *42*, 1081–1090.
14. Arzt, E.; Gorb, S.; Spolenak, R. From Micro to Nano Contacts in Biological Attachment Devices. *Proc. Natl. Acad. Sci. U.S.A.* **2003**, *100*, 10603–10606.
15. Varenberg, M.; Gorb, S. A Beetle-Inspired Solution for Underwater Adhesion. *J. R. Soc., Interface* **2008**, *5*, 383–385.
16. Autumn, K.; Liang, Y. A.; Tonia Hsieh, S.; Zesch, W.; Chan, W. P.; Kenny, T. W.; Fearing, R.; Full, R. J. Adhesive Force of a Single Gecko Foot-Hair. *Nature* **2000**, *405*, 681–685.
17. Autumn, K.; Sitti, M.; Liang, Y. A.; Peattie, A. M.; Hansen, W. R.; Sponberg, S.; Kenny, T. W.; Fearing, R.; Israelachvili, J. N.; Full, R. J. Evidence for van der Waals Adhesion in Gecko Setae. *Proc. Natl. Acad. Sci. U.S.A.* **2002**, *99*, 12252–12256.
18. Yurdumakan, B.; Raravikar, N. R.; Ajayan, P. M.; Dhinojwala, A. Synthetic Gecko Foot-Hairs From Multiwalled Carbon Nanotubes. *Chem. Commun.* **2005**, *30*, 3799–3801.
19. Mengüç, Y.; Yang, S. Y.; Kim, S.; Rogers, J. A.; Sitti, M. Gecko-Inspired Controllable Adhesive Structures Applied to Micromanipulation. *Adv. Funct. Mater.* **2012**, *22*, 1246–1254.
20. Liu, K.; Du, J.; Wu, J.; Jiang, L. Superhydrophobic Gecko Feet with High Adhesive Forces towards Water and Their Bio-Inspired Materials. *Nanoscale* **2012**, *4*, 768.
21. Vasav, S.; Blackledge, T. A.; Dhinojwala, A. Viscoelastic Solids Explain Spider Web Stickiness. *Nat. Commun.* **2010**, *1*, 19.
22. Opell, B. D.; Hendricks, M. L. The Role of Granules within Viscous Capture Threads of Orb-Weaving Spiders. *J. Exp. Biol.* **2010**, *213*, 339–346.

23. Opell, B. D.; Hendricks, M. L. Adhesive Recruitment by the Viscous Capture Threads of Araneoid Orb-Weaving Spiders. *J. Exp. Biol.* **2007**, *210*, 553–560.
24. Zhang, R.; Zhang, Y.; Zhang, Q.; Xie, H.; Wang, H.; Nie, J.; Wen, Q.; Wei, F. Optical Visualization of Individual Ultralong Carbon Nanotubes by Chemical Vapour Deposition of Titanium Dioxide Nanoparticles. *Nat. Commun.* **2013**, *4*, 1727.
25. Song, C.; Zhao, L.; Zhou, W.; Zhang, M.; Zheng, Y. Bioinspired Wet-assembly Fibers from Nanofragments to Microhumps on String in Mist. *J. Mater. Chem. A* **2014**, *2*, 9465–9468.
26. Reneker, D. H.; Yarin, A. L.; Fong, H.; Koombhongse, S. J. Bending Instability of Electrically Charged Liquid Jets of Polymer Solutions in Electrospinning. *J. Appl. Phys.* **2000**, *87*, 4531–4547.
27. Gong, G.; Wu, J.; Liu, J.; Sun, N.; Zhao, Y.; Jiang, L. Bioinspired Adhesive Superhydrophobic Polyimide Mat with High Thermal Stability. *J. Mater. Chem.* **2012**, *22*, 8257–8262.
28. Gong, G.; Gao, K.; Wu, J.; Sun, N.; Zhou, C.; Zhao, Y.; Jiang, L. A Highly Durable Silica/Polyimide Superhydrophobic Nanocomposite Film with Excellent Thermal Stability and Abrasion-Resistant Performance. *J. Mater. Chem. A* **2015**, *3*, 713–718.